3D FEMUR RECONSTRUCTION USING A ROBOTIZED ULTRASOUND PROBE

Pedro M. B. Torres⋆‡   *J. Miguel Sanches*†   *Paulo J. S. Gonçalves*⋆‡   *Jorge M. M. Martins*‡

⋆ Polytechnic Institute of Castelo Branco, School of Technology,
†Institute for Systems and Robotics, Bioengineering Department,
‡IDMEC / CSI, Mechanical Department,
Instituto Superior Técnico/ Tecnical University of Lisbon.
email: {pedrotorres|paulo.goncalves}@ipcb.pt,
{jmrs|JorgeMartins}@ist.utl.pt

ABSTRACT

Three-dimensional reconstruction of images is a fundamental procedure in medical imaging because it allows to build virtual models of anatomical units of the human body, useful in several areas, such as in surgical navigation. This paper presents a non free-hand Ultrasound acquisition system for human femur reconstruction where the probe displacement and position are accurately controlled by an anthropomorphic arm robot. The aim of this system is to acquire a sequence of 2D parallel cross-sections evenly spaced along the displacement direction in order to perform an accurate 3D reconstruction of the femur to be used in the scope of computer-assisted orthopedic surgery. Here, the system is described as well as the image processing and calibration procedures implemented. Results with real data are presented to illustrate the operation of the system.

Index Terms— Image-guided surgery, 3D surface reconstruction, Robotics

I. INTRODUCTION

Nowadays, robots are seen as a useful tool in an operating room and an indispensable collaborator when precision and accuracy are wanted in surgical procedures. There are many areas where medical tele-operated robots are found, e.g., laparoscopy, neurosurgery or orthopedic surgery. Robot examples are DaVinci, DLR MIRO [1], ROBODOC , among many others. In computer-assisted orthopedic surgery CAOS, fiducial markers are used to record the location of the bone with respect to the computer device, according to the

preoperative planning. This method, used by the ROBODOC system, has brought some problems, since it is necessary to pre-implant fiducial markers in the bone, through bone incisions. Studies on the operated patients reported persistent severe pain at the site of pin implantation, after surgery, which experts say are caused by the injuries to the nerves caused by these fiducial markers [2]. In order to avoid such problems and contribute to a minimally invasive surgery the HIPROB project has emerged, which is the development of a robotic arm co-manipulated by the surgeon for Hip Resurfacing surgery. The image-guidance system to control the robot navigation is based on ultrasound (US) images, eliminating the fiducial markers and reducing the complexity of the surgical procedure. Ultrasound is a non-invasive procedure, very safe, does not involve ionizing radiation and provides real-time imaging, making it a great tool for guiding the robotic system. However, there are a number of difficulties associated with the US data: speckle noise, saturation of the reflected echo at the bone-tissue boundary and ultrasound does not penetrate bone well, so only the outer surface of bone can be visualized. All of these factors must be carefully taken into account not to compromise the accuracy of the system [3]. Surgical navigation is based on computerized- tomography (CT) 3D data of the femur acquired in a pre-operative scenario. US data, acquired during the surgical intervention is used to align the CT data according to the position of the patient. To do this, a registration procedure between both data sets is performed [4] [5]. Here, parallel and evenly spaced US cross-sections of the femur are acquired with a robot arm and a 3D reconstruction is performed to be registered with the CT data previously acquired for surgical navigation purposes. This paper is organized as follows. In section II, the concept of automatic acquisition of US images are presented. The next section describes the US image processing steps. Section IV, describes the experimental evaluation and results. Finally,

conclusions and future work are presented.

II. AUTOMATIC ACQUISITION OF ULTRASOUND IMAGES

Recently, much scientific work has been produced in order to acquire ultrasound images with the aid of automatic mechanisms, such as robots [6] [7]. The concept of Ultrasound Visual Servoing [8] [9] is a theme that has shown good results in the control of probe positioning, with practical application in different areas, helping technicians and automating the diagnosis based on ultrasound images. Using a robot to move the probe, allows knowing the precise position and orientation (pose) in the workspace. The main objective of this work is to perform 3D reconstruction of a surface through US images. With the proposed system, it is possible through the homogeneous transformation matrix, obtained from the robot, to know the pose of each pixel in all images, without resorting to auxiliary equipment for spatial location. Each image is processed in terms of rotation and translation according to the homogeneous matrix:

$$HT = \begin{bmatrix} R_{3\times3} & t_{3\times1}[mm] \\ 0_{3\times3} & 1 \end{bmatrix}$$

In an automatic positioning system it is necessary to determine the relationship between the terminal element, where is coupled the probe, and the reference coordinate system. In this paper, a robot with 5 degrees of freedom (DOF) was used to move automatically the probe. The homogeneous transformation relating the tool frame to the fixed base frame is given by:

$$^{0}T_E = ^{0}T_1 \times ^{1}T_2 \times ^{2}T_3 \times ^{3}T_4 \times ^{4}T_5 \times ^{5}T_E \qquad (1)$$

where $^{i-1}T_i$ is the transformation between 2 consecutive links.

II-A. System Calibration

The estimation of the hand-eye and the robot-world transformations, to know the positioning of the probe at every moment, is an important point of this work. These estimations allow to perform a precise three-dimensional reconstruction of the bone. Figure 1 shows the necessary transformations. The transformation between the position coordinates of the world and the base of the robot (T0), and the transformation between the base of the robot and its end-effector, computed from the robot kinematics (T1), the transformation between the end-effector and the probe support (T2), the transformation between the probe support and the probe (T3), and the transformation from pixels to mm in the images frame (P) are needed to calibrate de system, according to:
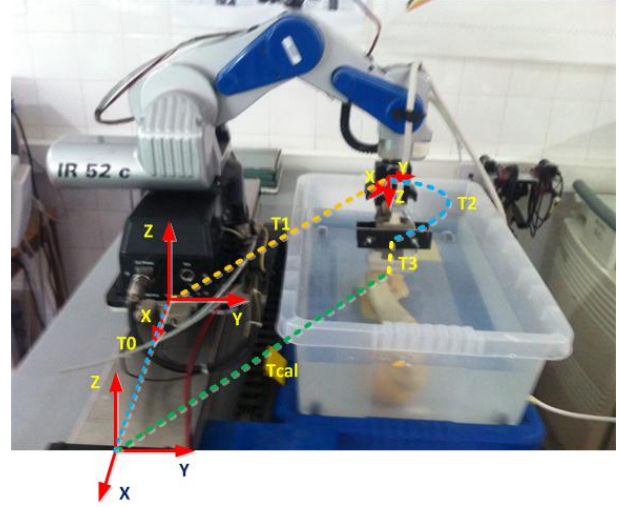

Fig. 1. Robot with frames used in calibration.

$$T_{cal} = T_0 \times T_1 \times T_2 \times T_3 \times P(u,v) \qquad (2)$$

where,

$$P(u,v) = \begin{bmatrix} S_x u \\ S_y v \\ 0 \\ 1 \end{bmatrix}$$

S_x and S_y are the scale factors for the (u,v) pixel coordinates. CIRS Ultrasound Calibration Phantom was used to obtain the scale factors to be used in $P(u,v)$. This Phantom is a cube with a small egg and a large egg. There are two scanning surfaces and the targets are centered within the background material. Knowing the dimensions of each egg, it is possible to obtain the relationship $pixels/mm$ for each level of depth of the US equipment and calculate the scale factors.

III. ULTRASOUND IMAGE PROCESSING

Since the bone is a rigid anatomical structure, ultrasound signals are reflected, and the image only captures the top layer of the bone. Processing this type of images is a challenging task, since images are very noisy and blurred. The image quality decreases severely when approaching the knee, because there is less muscle mass. The bone gets closer to the probe, so the US reflections are more intense. Other issue is the difficulty of coupling the probe to the knee, reducing the image quality. Cleaning the images without losing information is a very important point and a critical issue in the navigation based in US images. Image *Denoising* was used to remove the noise that degrades the images, for example Speckle, the most common noise in US images. The objective is to smooth homogeneous areas while

preserving the contours without distorting the images. There are several techniques to perform the $Denoising$ of images, as described in [10], [11] and [12]. Algorithm described in [12] was used. This algorithm uses the maximum a posteriori (MAP) criterion with a total variation (TV) edge-preserving Gibbs prior. The method is formulated as an optimization task that is solved by the Sylvester equation [12]. In order to speedup the processing time of the sequence, the initialization of the iterative filter at each image is performed by use of the previous denoised image in the sequence.
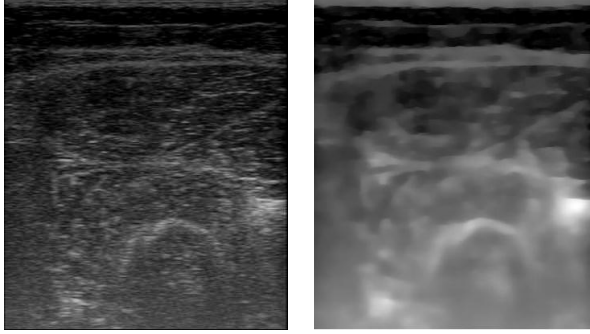

Fig. 2. a) Bone Ultrasound Image b) Denoised Image.

The alignment of consecutive images, slices, is another important issue, because allows to compensate possible probe displacement errors and leg movements. Normalized Cross-Correlation, described in [13], was used to align all ultrasound images, through equation 3.

$$\gamma(u,v) = \frac{\sum_{x,y}[f(x,y)-\overline{f}_{u,v}][t(x-u,y-v)-\overline{t}]}{\{\sum_{x,y}[f(x,y)-\overline{f}_{u,v}]^2 \sum_{x,y}[t(x-u,y-v)]-\overline{t}^2\}^{0.5}}, \quad (3)$$

where, f is the image, $\overline{t}$ is the mean of the feature and $\overline{f}_{u,v}$ is the mean of $f(x,y)$ in the region under the feature.

III-A. Image Segmentation

In this section, bone segmentation from the noiseless but blurred image (see Figure 2) produced in the previous section is described. There are several techniques for ultrasound image segmentation [14] [15] [16], and depending on the

Fig. 3. Example of Images Alignment. a) Image 1, b) Image 2, c) Image 2 aligned with 1.
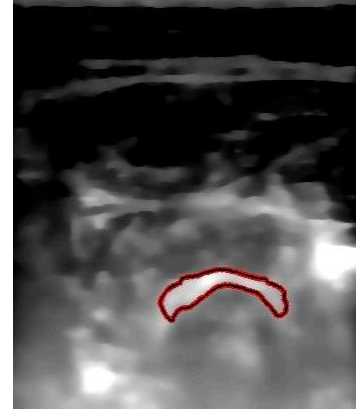

Fig. 4. Bone surface segmentation.

application an algorithm should be chosen or developed. For extracting contours in images of considerable complexity as ultrasound images, two families of methods have been extensively used by the image processing community, energetic (active contour models [17]) and probabilistic methods [18]. Here, the segmentation method described in [19], designed in the Geometric Active Contour framework and formulated as an optimization procedure, is used. The method assumes that the image is composed of two homogeneous regions referred to as "Object" and "Background". In the first step, the user provides an initial curve C within the region of interest representing a distance function $\phi : R^2 \rightarrow R$, where $\phi < 0$ represents the inside of C and $\phi > 0$ represents the outside of C. The goal is to evolve the curve C, or equivalently ϕ, so that the interior matches the "Object" and the exterior matches the "Background". The general minimization is performed by evolving C according to the flow:

$$\frac{\partial \phi}{\partial t} = \nabla_\phi E_{image} + \lambda.\delta(\phi).div(\frac{\nabla(\phi)}{|\nabla(\phi)|}) \quad (4)$$

where,

$$E_{image}(z,\phi) = \sqrt{\varepsilon\{(\log \frac{p_{in}(z,\phi)}{p_{out}(z,\phi)})^2\} - \varepsilon\{(\log \frac{p_{in}(z,\phi)}{p_{out}(z,\phi)})\}^2} \quad (5)$$

$\varepsilon \{f(z)\}$ is the expected value of the functional $f(z)$ with respect to the random photometric variable z. p_{in} and p_{out} are the probability density functions defined on the random variable z.

IV. EXPERIMENTAL EVALUATION

To validate the process, B-mode 2D ultrasound images of a human femur, 720×576 pixels were acquired. The robotic system used, consists of an $Eurobtec\ IR52C$ robot manipulator, an $ALOKA\ prosound$ 2 echograph with a $5MHz$ probe and a computer with a standard video card for image

acquisition. The probe is placed in the end effector of the robot, responsible for positioning the probe in contact with the leg. The images were acquired and the femur scanned with the best possible coupling at a constant speed. In the experiments performed, a 18 [cm] girl leg was scanned, on the central part of the leg from the hip to the knee. 297 images were acquired, meaning that the spacing among images is 0.6061 [mm]. To clean the images, a $Denoising$ algorithm described in section III was used in this work. Figure 2 shows an US image relate to a central area of the leg and the corresponding $Desoising$ result. Images alignment was obtained by maximizing the correlation among images. As depicted in figure 3, the image 2, was automatically shifted on the x and y axis, to coincide with image 1. The segmentation method described in section III-A was applied to all images. The initialization method is defined with a curve around the bone, identified by the user in the first image. After initialization, the algorithm automatically evolved to maximize the cost function. Figure 4, represents an example of bone segmentation. In this case the algorithm converges in 23.9094 seconds, after 300 iterations, in a Intel Core 2 Duo, 2.27 GHz computer, with 4 GB RAM. Using the segmented images, an isosurface is rendered and a surface was reconstructed using the well known $Marching$ $cubes$ [20] algorithm. Three-dimensional visualization of the femur allows to have a sense of its shape, identifies points of interest and subsequent registration with CT surfaces, and guides the surgeon and robot during surgical procedures. Figure 5 shows the 3D reconstruction surface of central part of the femur, where the images were acquired.

V. CONCLUSIONS

This paper describes a system for 3D reconstruction of the human femur from parallel and evenly spaced US cross sections acquired with a robot arm. Using this procedure is guaranteed the same pose of the probe and maintain the 3D orientation of each image slice, when moving the robot in the z direction. The location of each pixel of the image is obtained through a calibration process, that calculates the transformation matrices through direct kinematics of the robot, taking into account the probe attached to the robot hand rigidly. Ultrasound image processing was the critical task of this work, because the bone is a rigid anatomical structure that reflects US signals and the captured images represent only the upper surface of the bone. A method to $Denoise$ the US images, using a Bayesian algorithm based on a multiplicative model for the noise, is used. A geometric active contour based method, applied to 297 pre-processed images, shows its ability to reconstruct the bone surface. Having the bone contours in the 297 images and knowing the 3D position of each contour point, obtained from the robot, the marching cubes algorithm was applied to obtain the 3D model of the bone surface. As future work is expected to improve the US image segmentation process and perform

Fig. 5. Bone surface Reconstruction.

the registration between US images and CT images of the bone. The results obtained in this paper will be compared to the ones obtained using a spatial localizer.

VI. REFERENCES

[1] U. Hagn, M. Nickl, S. Jörg, G. Passig, T. Bahls, A. Nothhelfer, F. Hacker, L. Le-Tien, A. Albu-Schäffer, R. Konietschke, M. Grebenstein, R. Warpup, R. Haslinger, M. Frommberger, and G. Hirzinger, "The dlr miro: a versatile lightweight robot for surgical applications," *Industrial Robot: An International Journal*, vol. 35, no. 4, pp. 324–336, 2008.

[2] M. Nogler, H. Maurer, C. Wimmer, C. Gegenhuber, C. Bach, and M. Krismer, "Knee pain caused by a fiducial marker in the medial femoral condyle: a clinical and anatomic study of 20 cases.," *Acta orthopaedica Scandinavica*, vol. 72, no. 5, pp. 477–80, Oct. 2001.

[3] P. Penney, D. Barratt, C. Chan, M. Slomczykowski, T. Carter, P. Edwards, and D. Hawkes, "Cadaver validation of intensity-based ultrasound to ct registration.," *Medical image analysis*, vol. 10, no. 3, pp. 385–95, June 2006.

[4] D. Simon, "What is registration and why is it so important in caos?," *Engineering in Medicine*, 1997.

[5] P. Torres, P. Goncalves, and J. Martins, "Bone registration using a robotic ultrasound probe," *Proceedings of the III ECCOMAS Thematic Conference on Computational Vision and Medical Image Processing, VIPIMAGE2011*, 2011.

[6] P. Abolmaesumi, E. Salcudean, and H. Zhu, "Visual servoing for robot-assisted diagnostic ultrasound," *En-*

gineering in Medicine and Biology Society. Proceedings of the 22nd Annual International Conference of the IEEE, vol. 4, pp. 2532 – 2535, 2000.

[7] R. Mebarki, A. Krupa, and F. Chaumette, "2-d ultrasound probe complete guidance by visual servoing using image moments," *IEEE TRANSACTIONS ON ROBOTICS*, vol. 26,N.2, pp. 296–306, April 2010.

[8] R. Mebarki, A. Krupa, and F. Chaumette, "Image moments-based ultrasound visual servoing," *IEEE International Conference on Robotics and Automation, Pasadena, CA, USA*, pp. 19–23, May 2008.

[9] W. Bachta and A. Krupa, "Towards ultrasound image-based visual servoing," *Proceedings of the 2006 IEEE International Conference on Robotics and Automation, Orlando, Florida*, May 2006.

[10] A. Achim, A. Bezerianos, and P. Tsakalides, "Wavelet-based ultrasound image denoising using an alpha-stable prior probability model," *Computer Engineering*, 2001.

[11] N. Cumming, M. Sharkey, D. Plant, and G. Coulthard, "Subcutaneous erythropoietin alpha (eprex) is more painful than erythropoietin beta (recormon)," *Nephrology Dialysis Transplantation*, vol. 13, no. 3, Mar. 1998.

[12] J. Sanches, J. Nascimento, and J. Marques, "Medical image noise reduction using the sylvester-lyapunov equation," *IEEE transactions on image processing*, vol. 17, no. 9, pp. 1522–39, Sept. 2008.

[13] P. Lewis, "Fast normalized cross-correlation," *Industrial Light & Magic*, 1995.

[14] V. Fiete, S. Anand, and V. Kumar, "Current trends in segmentation of medical ultrasound b-mode images : A review," *Iete Technical Review*, vol. 26, no. 1, 2009.

[15] S. Alimohamadi, P. Farnia, J. Bidgoli, and A. Ahmadian, "An efficient extraction of bone surface using diffusion filters in ultrasound images of frontal bones," *Proceedings of the 11th International Conference on Information Sciences, Signal Processing and their Applications*, 2011.

[16] M. Talebi, A. Ayatollahi, and A. Kermani, "Medical ultrasound image segmentation using genetic active contour," *Biomedical Science and Engineering*, vol. 4, pp. 105–109, 2011.

[17] M. Kass, A. Witkin, and D. Terzopoulos, "Snakes: Active contour models," *International Journal of Computer Vision*, vol. 26, 1988.

[18] S. Jardim and M. Figueiredo, "Segmentation of fetal ultrasound images," *Medicine*, vol. 31, no. 2, pp. 243–250, 2005.

[19] R. Sandhu, T. Georgiou, and A. Tannenbaum, "A new distribution metric for image segmentation," in *SPIE Medical Imaging*. 2008, vol. 3, Citeseer.

[20] W. Lorensen and H. Cline, ""marching cubes: A high resolution 3d surface construction algorithm"," *ACM Computer Graphics*, vol. 21, no. 4, pp. 163–169, 1987.